Acta Geotechnica
https://doi.org/10.1007/s11440-024-02335-7

RESEARCH PAPER

Compacted sand–bentonite mixtures for the confinement of waste landfills

Robeta Proia[1] · Erminio Salvatore[2] · Paolo Croce[2] · Giuseppe Modoni[2]

Received: 14 July 2023 / Accepted: 24 March 2024

Abstract
This paper illustrates the results of an experimental study on sand–bentonite mixtures for their use as confinement barriers for solid waste landfills. The mixtures have been prepared parametrically varying the percentage of bentonite. The sample preparation method was established willing to simulate the compaction processes on site. In fact, the compacted samples were tested following two different stress-wetting paths representative of the possible stress and imbibition sequences occurring on a landfill confinement barrier. In the first case, the barrier comes into contact with rainwater before being subjected to the overloading stress induced by waste disposal, while, in the second case, the barrier is overloaded by the waste before being wetted by the leachate. The compressibility and permeability of the sand–bentonite mixtures were determined, in both cases, by oedometric compression tests. The experimental results are analysed and compared in order to evaluate the influence of the bentonite content on the mechanical and hydraulic behaviour of the mixture. Interpretation of the results is also accomplished with a micro-mechanical investigation of the mixtures fabric. Suitable compositions of sand and bentonite are finally proposed for the design of effective confinement barriers.

Keywords Bentonite compaction · Bentonite swelling · Bentonite hydraulic conductivity · Compaction of sand–bentonite mixtures · Hydraulic conductivity of sand–bentonite mixtures · Oedometer test on bentonite · Oedometer test on sand–bentonite mixtures · Sand–bentonite mixtures · Swelling of sand–bentonite mixtures · Waste landfills confinement

1 Introduction

It is generally agreed that correct waste management must promote the reuse and recycling of the waste itself, in order to reduce the disposal rates. Nevertheless, waste landfills still play a fundamental role in the management strategy of the waste cycle. Different rules and regulations have thus been developed in most countries to ensure safe and effective operation of landfills. Among various requirements, isolation of the waste body from the natural environment must be guaranteed by waterproofing the landfills bottom. This goal is typically pursued with artificial confinement barriers, made up of geomembrane sheets (usually high-density polyethylene—HDPE) placed on top of a compacted clay layer [13]. The latter must be able to stop leachate flow in case of malfunctioning of the geomembrane caused by a defective welding or punching of the sheets or by any other reason. As an example, the Italian regulation establishes a minimum thickness for the clay layer of 100 cm and a hydraulic conductivity of the material not higher than 10^{-7} cm/s.

However, suitable clay soil might not be always available at acceptable distances from the landfill. Thus, it becomes necessary to use alternative materials that meet the same regulatory requirements. A possible solution consists in adding a hyperplastic material like bentonite, to

✉ Erminio Salvatore
e.salvatore@unicas.it

Robeta Proia
roberta.proia@isprambiente.it

Paolo Croce
croce@unicas.it

Giuseppe Modoni
modoni@unicas.it

[1] ISPRA Istituto Superiore Per La Protezione E La Ricerca Ambientale, Via V. Brancati 48, 00144 Rome, Italy

[2] Department of Civil and Mechanical Engineering, University of Cassino and Southern Lazio, Via G. Di Biasio 43, 03043 Cassino, Italy

Published online: 17 May 2024

granular materials available on site, in order to infer a waterproofing capacity to the latter [8, 13, 34, 54]. The principle of sand–bentonite mixtures stands in mixing two materials that are chemically stable and currently available from the mining industry, to combine their largely different physical, hydraulic and mechanical properties in a new product able to accomplish the isolation requirements. Bentonite is a very active clayey material that infers a low permeability and a high ductility to the mixture, allowing to control seepage and undergo large deformations without cracking [34]. Sand is a granular material capable of forming a relatively stiff and strong fabric. In addition, it provides stability against the swelling–shrinkage tendency of the bentonite when the latter is subjected to cyclic wetting–drying processes [9, 11, 53]. Cut-off walls for hydraulic or waste-containment facilities [14], impervious cores of earth dams [23] or barriers to the seepage at the base of waste landfills [13] are among the typical applications of the sand–bentonite mixtures. In the past, this material has also been exploited to seal nuclear waste disposals [22]. More recently, El Mohtar et al. [12] and Santagata et al. [37] have shown the capability to reduce the liquefaction susceptibility by permeating bentonite suspensions through the sand pores.

Each application is characterized by a variable amount of bentonite, water and a different construction method. In particular, cut-off walls are made by pouring the mixture as a slurry prepared with very high water content, while earth dams' cores and landfills base layers are created with mechanical compaction at much lower water contents [13, 14]. For each case, it is necessary to understand the working conditions to set a material's composition that enhances the required functions. In general, the waterproofing capacity of the bentonite can be associated with the relatively high shear strength typical of sand, being the material's composition a fundamental design issue. If the swell capacity of the bentonite exceeds the void space available among the sand grains, the pores are completely filled with hydrated bentonite and the permeability of the mixture becomes very low, approaching the characteristic value of bentonite [20]; on the other hand, if the bentonite content is too small, the sand pores are not completely filled and water is able to seep with relative freedom. However, large amounts of bentonite reduce the material strength up to a point that the material might become unstable and compaction troublesome.

A review of case studies regarding the use of bentonite in earth dams shows typical percentages of bentonite ranging between 0.5 and 5% [20, 23, 52], whereas, in the case of liner systems used to reduce leakage of pollutants in waste disposal landfills, variable proportions are assigned with bentonite content varying from 15 to 100% [34].

The economic convenience of sand–bentonite mixtures for waste confinement barriers must be each time evaluated considering the amount of bentonite necessary to achieve the desired goal, in order to compare the costs of materials with those alternatively necessary to bring larger amounts of clayey soil from long distances. A comparison is not possible in absolute terms, as costs depend very much on local conditions, logistic issues (primarily the distance from quarries) and market (unit prices). However, the economic convenience of sand–bentonite barriers relies on the optimal setting of bentonite content which is among the goals of the present study. Bearing this goal in mind, the present study covers the full range of bentonite content (from 0 to 100%), focusing on the properties of this composite material relevant for confining solid waste landfills. The transition from the response of a granular to plastic material is studied looking at the properties that dictate the material's response in this specific application. Plasticity, compaction, compressibility, swelling and permeability are investigated to understand fundamental mechanisms and define an optimal composition. The experimental evidence noticed at the sample scale has then been interpreted with a microstructural investigation.

To verify the property of sand–bentonite mixtures for waste confinement, an extensive experimental study has been thus conducted. Laboratory investigations have been performed on samples prepared by mixing sand and bentonite with different proportions. Samples have been prepared reproducing the site compaction process induced by drum rollers. Hence, the compacted samples have been tested following two different stress-hydraulic paths, representing possible extreme wetting and loading sequences of the landfill bottom layer. In the first case, the confinement barrier comes into contact with rainwater soon after placement and is thus saturated before being subjected to the overloading stresses induced by waste placement. In the second case, it is assumed that the barrier is not wetted by rainwater during landfill construction and is thus overloaded in partially saturated conditions by the waste mass. This sand–bentonite layer could ultimately be saturated by the leachate produced by waste degradation (in the event of geomembrane malfunctioning).

Compressibility and permeability of the sand–bentonite mixtures have been determined, for both stress-wetting paths, by means of oedometric compression tests. Samples saturation is accomplished in both cases by adding distilled water. The experimental results are analysed and cross-compared in order to evaluate the influence of the bentonite content on the mechanical and hydraulic behaviour of the mixture. Suitable compositions of sand and bentonite are then proposed for the design of effective confinement barriers together with practical design considerations.

2 Physical properties

The materials used in the experimental investigation are a quarzitic sand from a quarry located in the area of Fossanova (Southern Italy) and a sodium bentonite quarried from Milos Island (Greece). The particle size distributions of both materials, obtained by standard sieving and sedimentation tests, are shown in Fig. 1.

The Fossanova sand is composed by subrounded grains having diameters ranging between 0.180 and 0.425 mm, uniformity coefficient equal to 1.54 and specific gravity equal to 2.65.

The Milos bentonite, composed by approximately 80% clay, 15% silt and 5% fine sand has a specific gravity equal to 2.83. X-ray diffractometry reveals montmorillonite to be the principal component of the bentonite [33].

The two materials are mixed in variable proportions, identifying each mixture with its bentonite content (BC) defined as the weight percentage of dry bentonite referred to the total dry weight of the mixture. Liquid limit (w_L) and plasticity index (PI) obtained for the different mixtures are plotted on the Casagrande plasticity chart of Fig. 2. As expected, the plasticity of the mixtures increases with the fraction of bentonite, as also shown by previous studies [42, 43]. In particular, the experimental data follow a linear trend along the U line, typical of montmorillonites [18] falling above the H line of high-activity materials [30, 31]. It is also worth observing that small quantities of bentonite (BC = 5, 7 and 10%) affect the liquid limit of the material but do not infer meaningful effects on the plastic limit, which is zero for the above percentages and is measurable only for quantities of bentonite greater than 10%.

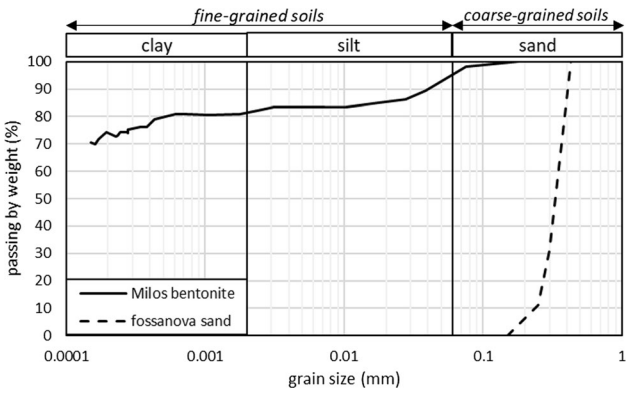

Fig. 1 Grain-size distribution curves of Fossanova sand and Milos bentonite used for preparing the mixtures

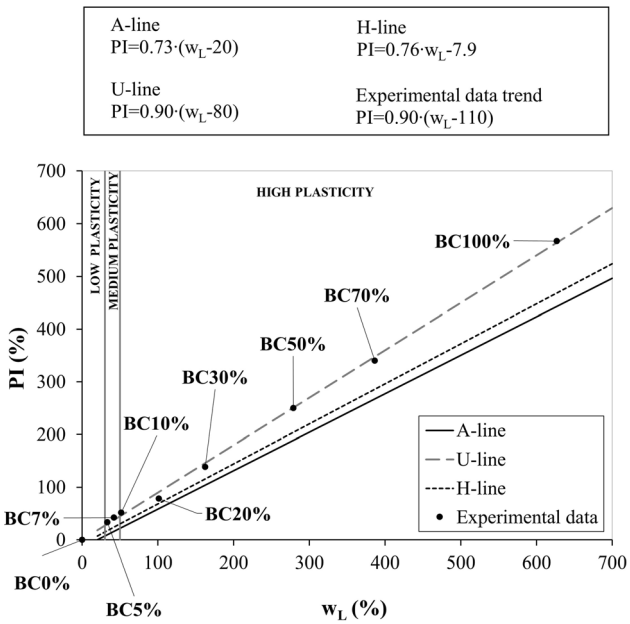

Fig. 2 Plasticity trend for increasing bentonite content (BC)

3 Sample preparation and compaction

In order to define the compaction characteristics of the mixtures [33], standard Proctor tests have been performed on materials prepared with a wide range of BC adopting the procedure named as b-method in the ASTM procedure [4]. Normally, the choice of Proctor test type, standard or modified, stems from a consideration on the energy involved in the examined application. The standard Proctor procedure has been preferred to the modified one considering that the lesser energy inferred on the sample enables to reach the maximum relative density at higher water contents and thus to better identify the contribution of the sample humidity.

The mixing of sand, bentonite and water was carried out following the instructions given by Kenney et al. [20] to form the most possible homogenous material. For low bentonite content (BC $\leq$ 30%), sand and bentonite were first mixed in a dry state and then water was gradually added while stirring the paste; for higher BC (> 30%), the above procedure did not guarantee homogeneity of the material and therefore the sand was firstly mixed with water, then dry bentonite was slowly added, carefully mixing the material with a spatula.

After mixing, the material was put in plastic bags and allowed to hydrate for about 24 h, then compaction tests were performed. For each BC, standard Proctor compaction tests [4] were accomplished for variable water contents in order to define a continuous compaction curve (dry unit weight, γ_d, vs. water content, w). The optimal compaction, defined as the maximum dry unit weights ($\gamma_{d,\max}$) and the

related water contents (w_{opt}), is evaluated for each mixture from the regression curves. The results of compaction tests, plotted in Fig. 3, can be summarized as follows:

- The density of the pure sand (BC = 0%) is dictated by its uniformity coefficient [19] and, as expected, does not depend on water content.
- The density of pure bentonite (BC = 100%) is much lower, being slowly influenced by the water content.
- The mixture prepared with the lowest bentonite content (BC = 5%) reaches a density higher than sand but compaction is still negligibly affected by the water content.
- All the mixtures with a bentonite content greater than or equal to 7% (BC $\geq$ 7%) show the classic bell-shaped compaction curve, with a well-defined optimal compaction point (w_{opt}–$\gamma_{d,max}$). Tatsuoka and Correia [47] point out the paramount role of saturation degree on the maximum density of clayey soils. According to this evidence, the controlling variable should be the saturation degree of the bentonite. Herein, it is not possible to decouple the water contents of bentonite and sand without making subjective assumptions. It was only possible to compute a saturation degree for the pure bentonite (BC = 100%) equal to 0.75, which is in line with the indication of Tatsuoka and Correia [47].

In Table 1, the physical properties and the compaction characteristics of each mixture are summarized.

The maximum Proctor density is now plotted versus the bentonite content in Fig. 4. The plot clearly shows that density increases with the bentonite content and reaches its maximum for BC$\approx$20%, then progressively decreases. This trend can be interpreted by identifying three different

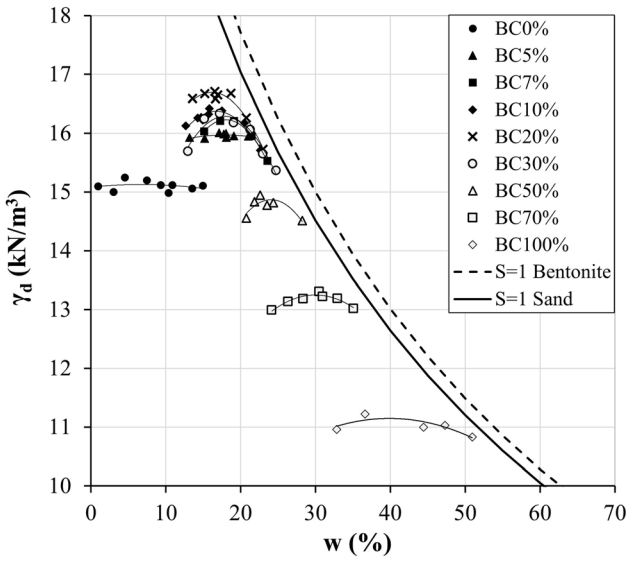

Fig. 3 Compaction curves of the sand–bentonite mixtures

fabric types of the sand–bentonite mixture considering the interparticle void ratio concept [49–51]. A "coarse matrix" structure (i.e. sandy structure) is obtained when the sandy matrix is predominant. This composition infers to the mixture a mechanical behaviour similar to that of a cohesionless soil (BC < 10%, area A in Fig. 4); on the other side, a "fine matrix" structure (i.e. clayey structure) is created for high percentages of bentonite, when the sand grains are dispersed within the clayey matrix. This composition induces a mechanical behaviour typical of a fine-grained material (BC > 50%, zone C in Fig. 4). A "combined fabric" occurs for intermediate compositions of the mixture, where it is presumed that both components contribute to the mechanical behaviour of the mixture (10% < BC < 50%, zone B in Fig. 4).

The theoretical value of the maximum dry density ($\gamma_{d,max(A)}$) for the sandy structure material can be computed with Eq. (1) as a function of the bentonite content (BC):

$$\gamma_{d,max(A)} = \frac{\gamma_{s,sand}}{e+1} \tag{1a}$$

where e represents the interparticle void ratio:

$$e = e_{g,min}\left(1 - \frac{BC}{100}\right) - \frac{BC}{100} \tag{1b}$$

This relation considers the void ratio corresponding to the maximum compaction of the pure sand ($e_{g,min}$ = 0.73, computed considering the above given sand specific gravity) and the partial filling of soil pores with the bentonite. The basic assumption behind this calculation is that the low content of bentonite does not interfere with the Proctor compaction of sand [49].

On the other side, for the clay structure, the maximum density of the mixture ($\gamma_{d,max(C)}$) can be correlated through Eq. (2) to the bentonite content (BC):

$$\gamma_{d,max(C)} = \frac{1}{\frac{e+\frac{BC}{100}}{\gamma_{s,bent}} + \frac{1-\frac{BC}{100}}{\gamma_{s,sand}}} \tag{2a}$$

where

$$e = e_{f,min} \times \frac{BC}{100} \tag{2b}$$

The minimum void index of the bentonite component ($e_{f,min}$ = 1.49 i.e. minimum interfine void ratio) corresponds to the maximum compaction of pure bentonite for the above given specific gravity. The basic assumption behind this calculation is that the low content of sand does not interfere with the Proctor compaction of bentonite.

Results obtained by Eqs. 1 and 2 are plotted on Fig. 4 with two dashed lines, intersecting at a point which defines the maximum theoretical value of the density of a mixture made up of two different single-granular components. This

Table 1 Physical properties and compaction characteristics of sand–bentonite mixtures

	Physical properties			Compaction characteristics		
BC (%)	w_L (%)	w_P (%)	PI (%)	w_{opt} (%)	γd_{max} (kN/m^3)	e_{min}
0	0.00	0.00	0.00	–	15.11	0.73
5	33.39	0.00	33.39	–	15.95	0.64
7	42.12	0.00	42.12	18.00	16.22	0.61
10	51.57	0.00	51.57	16.74	16.38	0.60
20	101.50	23.11	78.39	16.17	16.70	0.58
30	162.48	24.01	138.47	17.95	16.30	0.63
50	279.09	29.27	249.82	24.11	14.90	0.81
70	386.58	46.33	340.25	30.09	13.28	1.05
100	626.73	59.65	567.09	39.78	11.14	1.49

BC, bentonite content; w_L, liquid limit; w_P, plastic limit; PI, plasticity index; w_{opt}, optimum water content; $\gamma_{d,max}$, maximum dry unit weight; e_{min}, void ratio corresponding to maximum dry weight

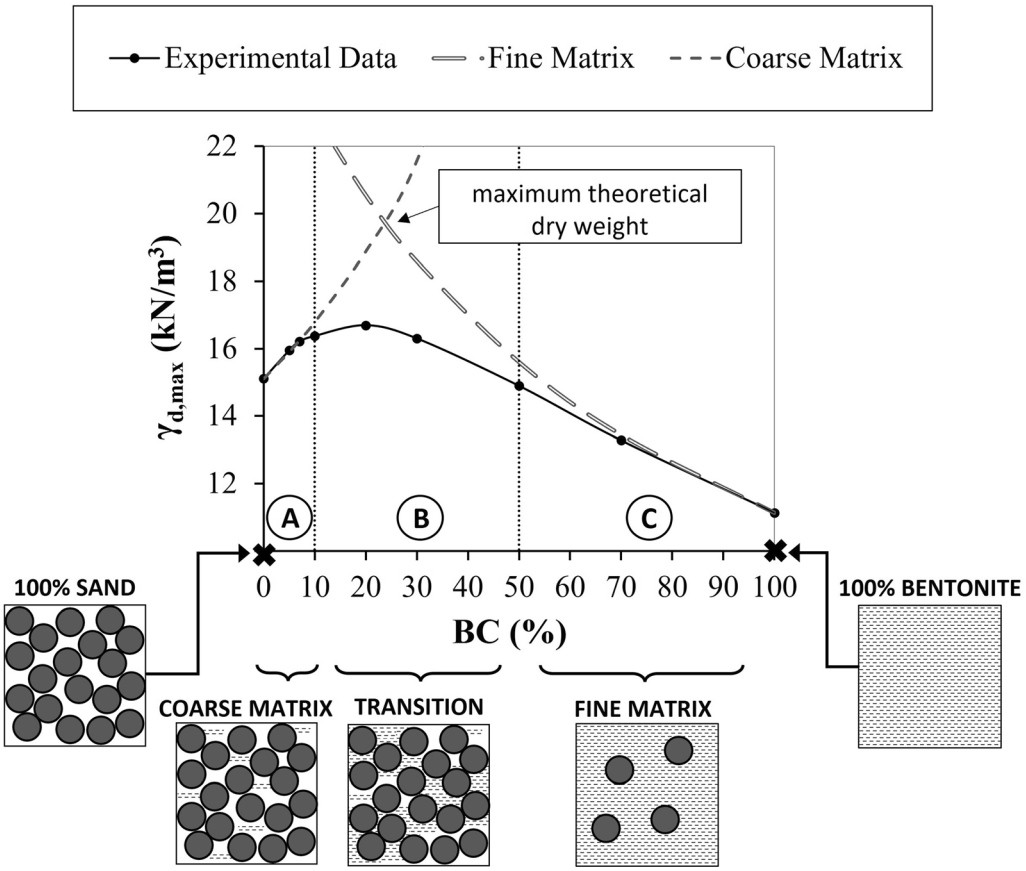

Fig. 4 Maximum dry density as a function of the bentonite content

highest value cannot be reached due to the complex interaction occurring between sand and bentonite during compaction, when neither of the two components is predominant. However, it is worth noting from the plot that the fabric of sand formed by compaction is not affected by the bentonite until BC exceeds values of 10%, while the fabric of the pure bentonite is limitedly affected by sand for contents of the coarse material lower that 40% (BC = 50 ÷ 60%). Interaction among the two components plays a role in the intermediate phase (named transition in Fig. 4).

The optimum water content w_{opt} and the corresponding saturation degree S are also plotted versus bentonite

content in Fig. 5. It is observed that the saturation degree varies randomly in a relatively narrow range (S = 0.73 ÷ 0.81), while the optimum water content varies substantially as a function of the bentonite content. In particular, a linear dependency of w_{opt} on BC can be inferred for materials with larger bentonite fractions, meaning that the compaction is basically dominated by the finer material. On the contrary, for relatively lower BC (5 ÷ 30%), w_{opt} is more stable, meaning that the bentonite plays a less important role or, at least, the response is also ruled by the sand.

The results from the present experiment are combined in Fig. 6 with the other literature data [2, 6, 39, 43]. Noting that the present experimental campaign is the only one accomplishing BC values higher than 50%, the comparison of w_{opt}–γd_{max} curves shows a similar response for all cases in spite of obvious differences on the swelling properties of the bentonite and on the grain size distributions of the sand. It is, however, noted that, while the dry density of the very uniform Fossanova sand starts from relatively low values, and thus bentonite has enough space to fill the pores without interacting with compaction, according to previous observation of Santucci De Magistris et al. [38], the same effect does not hold true for more heterogeneous materials (e.g. Shaker and Elkady [39]) able to reach higher density. Here, thanks to the lower volume of pores, bentonite starts to interact with compaction much earlier. This phenomenon has a relevant implication when defining the mixtures design, i.e. the composition that combines low permeability with stability.

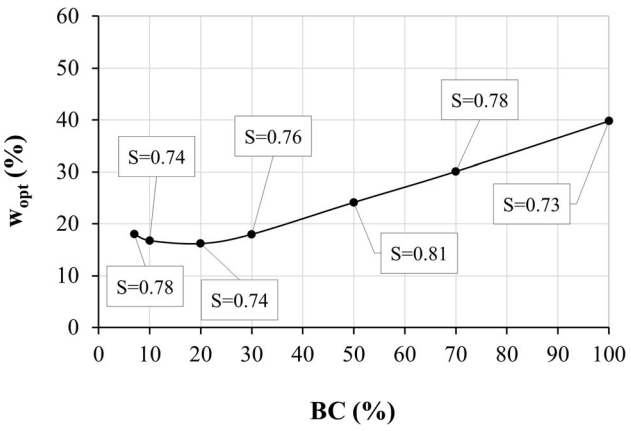

Fig. 5 Optimum water content (w_{opt}) and saturation degree (S) obtained by compacting sand–bentonite mixtures prepared with various bentonite contents (BCs)

4 Fabric of compacted mixtures

The three possible types of microstructural arrangement, just figured out from the results of compaction tests (Fig. 4), have now been observed with a microstructural investigation. To this aim, scanning electron microscopy (SEM) and mercury intrusion porosimetry (MIP) analyses have been performed on samples compacted with the standard Proctor procedure. It must be recalled that the microstructure of a material formed by granular and plastic particles is substantially affected by the water content. For homogeneity among the studied composition, but also consistently with a possible site application, all samples subjected to the microstructural analyses have been prepared at the optimum water content previously determined with the Proctor tests. More details on these tests are reported in [32].

It is necessary to point out that samples subjected to SEM were prepared after air drying and this procedure induced some shrinkage of the bentonite that masks its relevance on the overall soil fabric. However, the scanning reported in Fig. 7 clearly shows that for a low amount of bentonite (BC = 5%-Fig. 7b), the *coarse matrix* prevails, being the sand fabric only marginally affected by the addition of bentonite. It just starts filling the pores and partially coats the sand grains, but the material response is still dominated by the grain-to-grain contacts, thus confirming the evidences by the compaction curves (Fig. 4). Previous ESEM studies performed by Montanez [28] noticed a similar response. The role of bentonite on the whole response becomes progressively more important for higher bentonite contents. In fact, the bentonite paste adheres to the sand grains surface and forms bridges that affect the grain-to-grain contact force transmission (Fig. 7c, d). In the transitional zone, the mixtures show a complex microstructure, with a mechanical response partly dictated by the sand particles and their contacts, partly affected by the bentonite compression. For higher bentonite contents (Fig. 7e), the fine matrix response is predominant. Here, the sand grains are progressively less recognizable being fully surrounded by the bentonite matrix. This arrangement, partly masked in the figure by the shrinkage of the bentonite occurred upon drying, highlights the marginal role of floating sand particles on the mechanical response and compaction as well. The above evidences are consistent with the conceptual model depicted in Fig. 4 and previously envisaged by Thevanayagam et al., 2003 [49].

In the performed MIP investigation [26], freeze drying of the samples was performed to eliminate the pore water without modifying shape and dimension of the original pores [58]. Briefly, MIP tests consist in filling the soil pores with a very high surface tension fluid, the mercury,

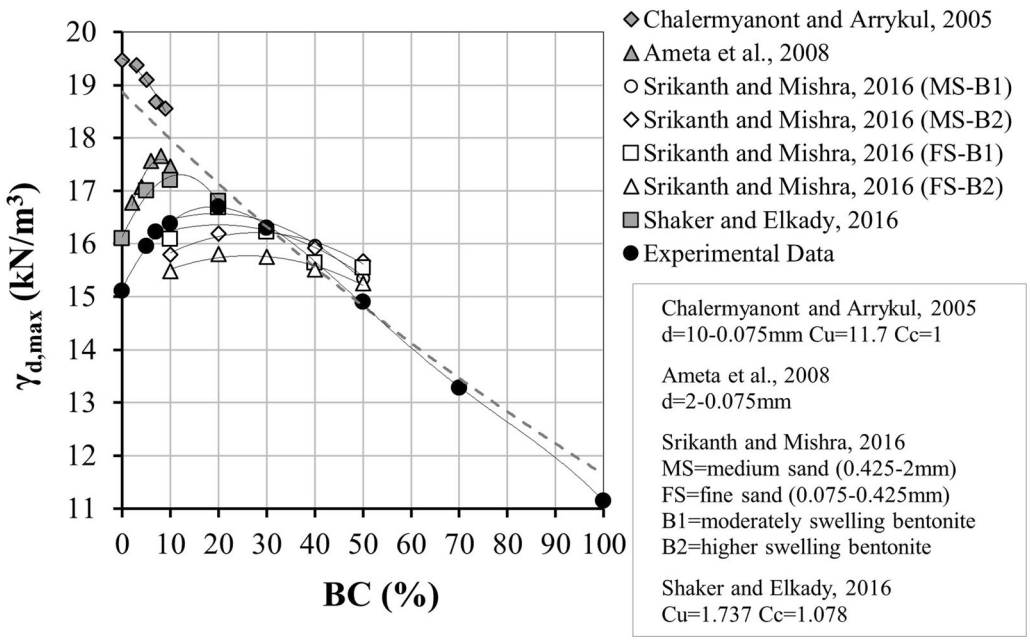

Fig. 6 Comparison with the literature data for compaction characteristics of sand–bentonite mixtures

progressively increasing the injection pressure in order to fill progressively smaller pores. Using a theoretical relation between injection pressure and pores size [56], it is possible to relate the amount of mercury cumulatively intruded in the material pores, proportional to the volume of voids (e_{MIP}), to the dimension of the occupied pores. Finally, the pore size density function PSD = $de_{MIP}/d(\log P)$ can be computed as a function of the pores size (d), which represents the distribution of volume fractions corresponding to each pore size. This analysis has been performed on sand–bentonite mixtures compacted at the optimum standard Proctor for $10\% \leq BC \leq 30\%$ (transition phase, see Fig. 4) and the curves are shown in Fig. 8.

All mixtures in the plot present a trimodal distribution. This result, also seen by Dixon et al. [10] despite their MIP tests were performed on oven-dried samples, implies that the microstructure of the material includes three families of pores with largely different dimensions and relative proportions: the macro-pores, having dimensions in the range 10–100 m, that represent the inter-grain spaces, i.e. the voids formed among the sand particles (whose diameters range between 0.180 and 0.425 mm Fig. 1) and free from the bentonite occupation; the mesopores, with dimensions in the order of few microns and a larger amount, represent the inter-cluster spaces, i.e. the voids intercluded among bentonite clusters; the micropores, with dimensions in the order centi-microns, represent the intra-cluster spaces, i.e. the voids entrapped within the bentonite clusters.

For completion, the presence of mesopores and micropores was already observed by previous investigations performed on compacted bentonite samples [35], and a bimodal distribution was observed on compacted sand–bentonite mixtures with high bentonite contents [1, 7, 25].

The distributions of the three pore classes obtained for materials with, respectively, BC = 10, 20 and 30% show some differences that deserve attention (Fig. 8). The presence of bentonite somehow affects the compaction of sand as slightly larger volumes of macropores (inter-grain) are seen for BC = 20 and 30% compared with BC = 10%. It was noticed before (Figs.4, 5 and 7) that, with these fractions, the material fabric is still influenced by sand, but the bentonite starts playing a progressively more relevant role on compaction (see the transition phase in Fig. 4). The macropores are partially filled by bentonite clusters, but the voids formed among them (mesopores) are the widest pore component. In terms of volume and dimensions, this volume is higher for the lowest bentonite content (BC = 10%) while tends to decrease for higher BC values. The increase of BC produces a progressive reduction of the volume and dimension of the inter-cluster voids (mesopores) possibly because, with higher bentonite fractions, compaction starts to act on the clusters entrapped in the grain spaces.

Finally, there seems to be no clear trend between amount of micropores and BC. In fact, while the volume of micropores increases for BC passing from 10 to 20%, it reduces for BC = 30%. Some role of the water–bentonite interaction on the fabric of the compacted soil could be envisaged [41], but data are too scarce to draw any conclusion.

As a general conclusion from both the above analyses, it is quite evident that for contents higher than 10%, there is a

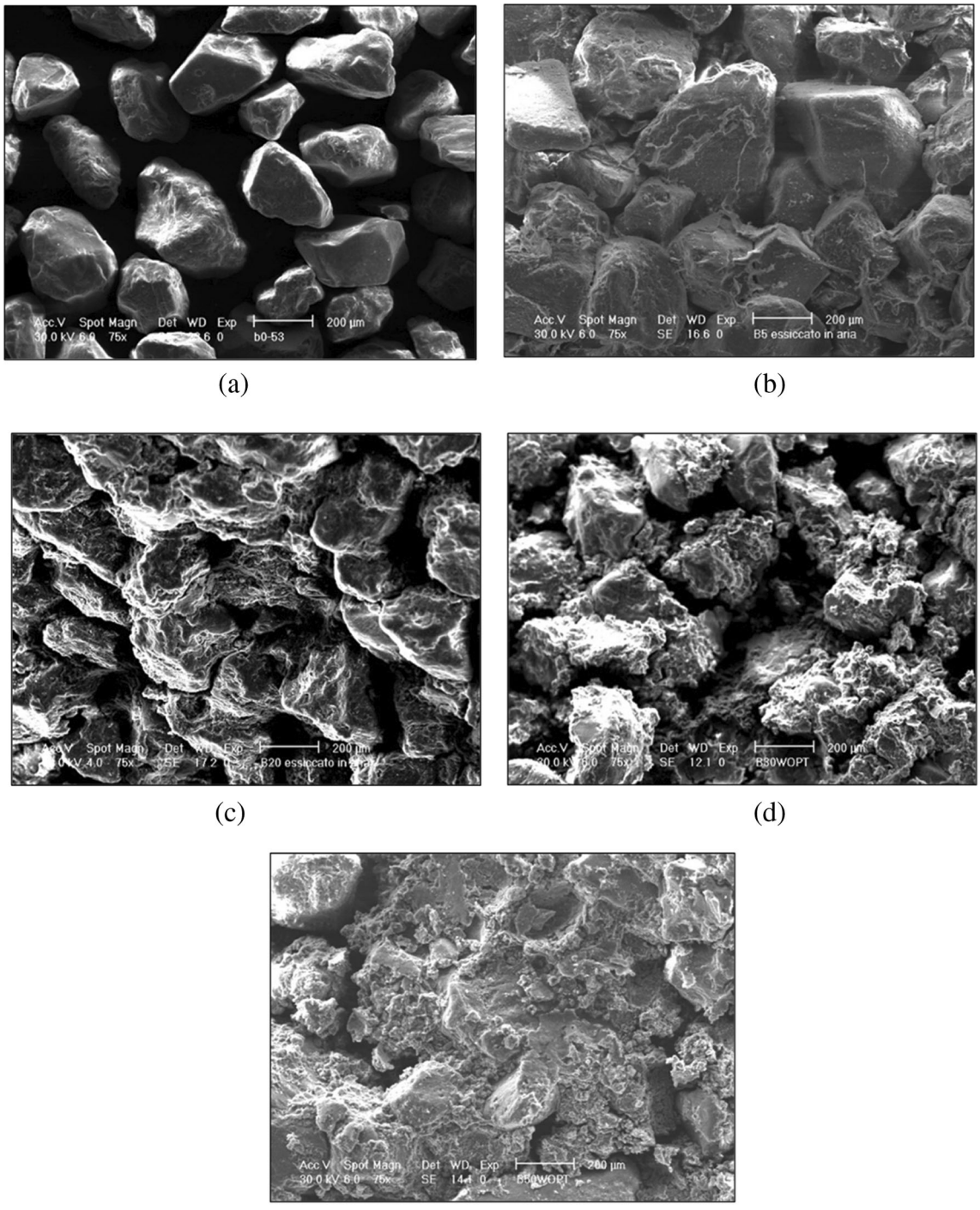

Fig. 7 SEM micrographs on oven-dried sample (**a** BC = 0%—γ_d = 14.99 kPa—w = 0.10; **b** BC = 5%—γ_d = 16.00 kPa—w = 0.18; **c** BC = 20%—γ_d = 16.59 kPa—w = 0.17; **d** BC = 30%—γ_d = 16.20 kPa—w = 0.18; **e** BC = 50%—γ_d = 14.74 kPa—w = 0.24)

transfer of compaction effects from the sand to the bentonite.

5 Swelling and compressibility

The compressibility of the mixtures was investigated by means of one-dimensional (i.e. oedometer) compression tests [3], performed with different procedures conceived to

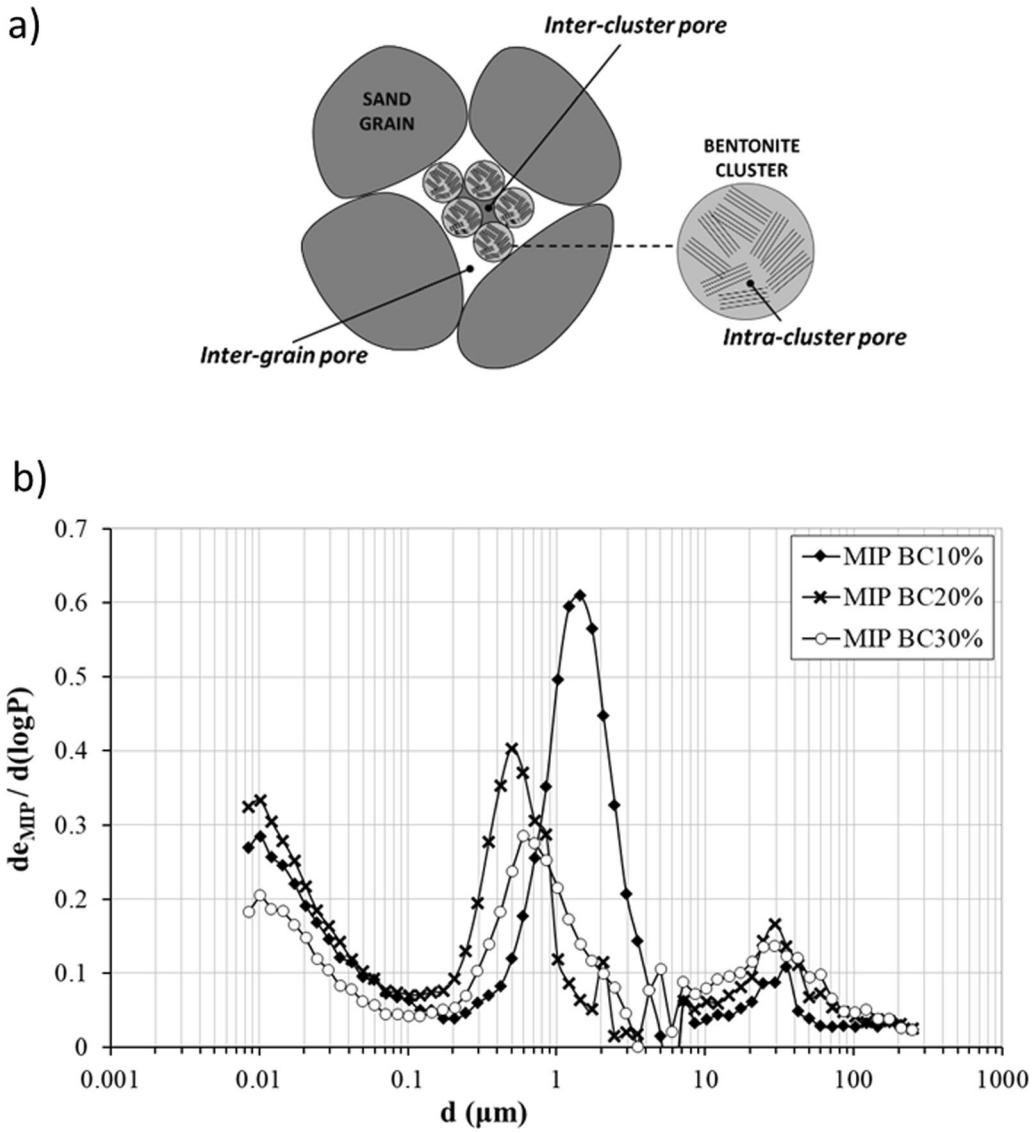

Fig. 8 Pore size density function (PSD = $de_{MIP}/d(\log P)$) versus pore diameter (d)

simulate the conditions that may occur at the bottom of a landfill (Fig. 9). In general terms, the application of sand–bentonite mixtures at the bottom of waste deposits implies compaction, soaking and loading induced by waste placement. The latter two steps normally occur simultaneously or, more rarely, with one phase anticipating the other. For instance, soaking may occur before waste placement due to heavy rainfall, or during and after waste placement due to leakage. In the present study, two extreme conditions have been considered, with soaking occurring up to saturation before load application, or loading applied on freshly compacted material and soaking occurring thereafter.

In the first case, it is assumed that the landfill bottom is saturated by rainwater before placing the waste and therefore the sand–bentonite layer can swell freely before being subjected to overloading. To simulate this first condition, the samples marked with the acronym CS (compacted-swelled) in Fig. 9 were first compacted to the Proctor's optimum state, then soaked with water up to saturation and left free to swell one-dimensionally in a confining ring until no more deformation was recorded. This process was accomplished on average in 29 days. Thereafter, the samples were transferred in the oedometer equipment and subjected to confined compression tests.

In the second case, it is assumed that landfill construction proceeds without infiltration of meteoric water and that imbibition takes place only subsequently due to the deferred production of the leachate. In this situation, swelling induced by the imbibition is counteracted by the weight of wastes and the final state is dictated by the comparison between the applied vertical loading and the swelling pressure. The former is proportional to the

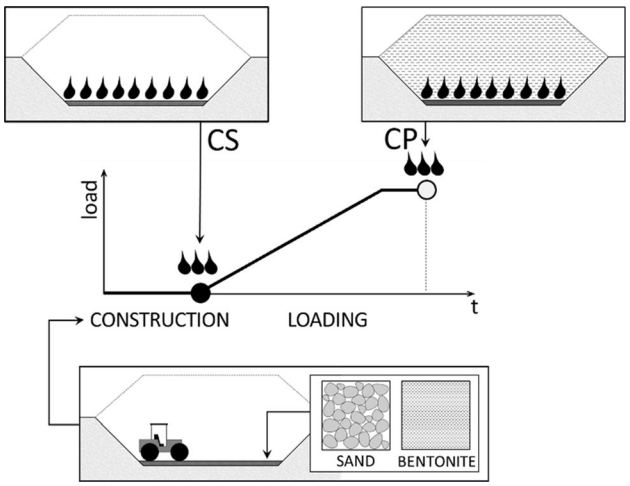

Fig. 9 Loading/wetting paths of the bottom barrier of a solid waste landfill

thickness of the deposit and thus depends on the specific application, the latter can be measured with an ad hoc laboratory procedure. In the present study, the swelling pressure has been inferred soaking the sample with water up to saturation directly in the oedometer cell while progressively increasing the vertical load in order to fully compensate swelling [17]. This process took about 26 days on average to finish. After reaching the swelling pressure, the oedometer tests were prolonged increasing the vertical load as in the previous case. These samples are marked with the abbreviation CP (compacted-prevented Swelling) introduced in Fig. 9. The main results obtained for both loading paths are summarized in the following figures.

The experimental evidence shows a good correspondence between swelling deformation of the CS samples (Fig. 10) and swelling counterbalancing pressure of the CP samples (Fig. 11). Both values increase with the bentonite content, in agreement with the previous literature studies [27, 44, 57]. It is also worth noting that swelling deformation and swelling pressure are practically zero for BC = 5% and start to increase for rather low BC (say less

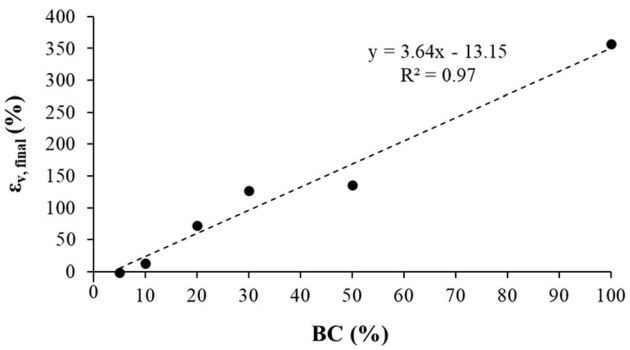

Fig. 10 Swelling of samples with CS path as a function of bentonite content

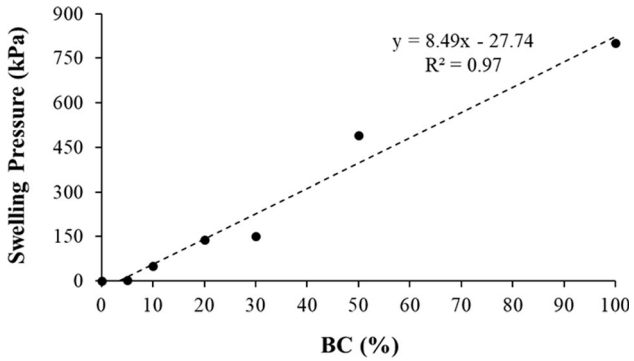

Fig. 11 Swelling pressure of samples with CP path as a function of bentonite content

than 10%). Considering water adsorption peculiar of the plastic materials, this result implies that bentonite swells within the sand pores, i.e. without affecting the fabric of mixture, for contents lower than 10%. For higher BC, swelling of the bentonite forces the sand fabric to expand, with particles moving away from each other. This result represents the other side of the medal with the evidence previously seen on compaction where the effect of bentonite was seen starting from BC approximately equal to 10% (Fig. 4).

The oedometer test results are summarized in Figs. 12 (from a to f for BC ranging between 0 and 50%) combining in each plot the results of samples left free to swell (path CS) with those of samples with prevented swelling (path CP) for different bentonite contents. A third set of results is added in the plot for reference, representing the compression curves of samples reconstituted in a fully saturated state without compaction following the procedure proposed by Burland [5]. It consists in adding to each mix a water content contained between 1 and 1.5 times the liquid limit to derive the curve in the e–σ_v plane defined by Burland as intrinsic compression line (ICL). In all plots, the ICL curve of the pure bentonite is also reported.

Considering the large compressibility of the bentonite, all curves are plotted on bi-logarithmic planes adopting the same scale [40]. In fact, the compression curves do not show the typical linear trend of the normal consolidation line when plotted on the classical e-log(σ'_v) plane, while are better interpolated by straight lines (characterized by high R^2 values) in the bi-logarithmic plane log(σ'_v)–log(e). It follows that the compressibility of the mixtures can be characterized by the index α included in the following relation Eq 3:

$$log(e) = \beta - \alpha \times log\sigma_{v'} \tag{3}$$

All curves for increasing BC values start from progressively larger initial void ratios being those obtained on slurry samples (S) always above those representative of free swelling samples (CS), the latter always above those

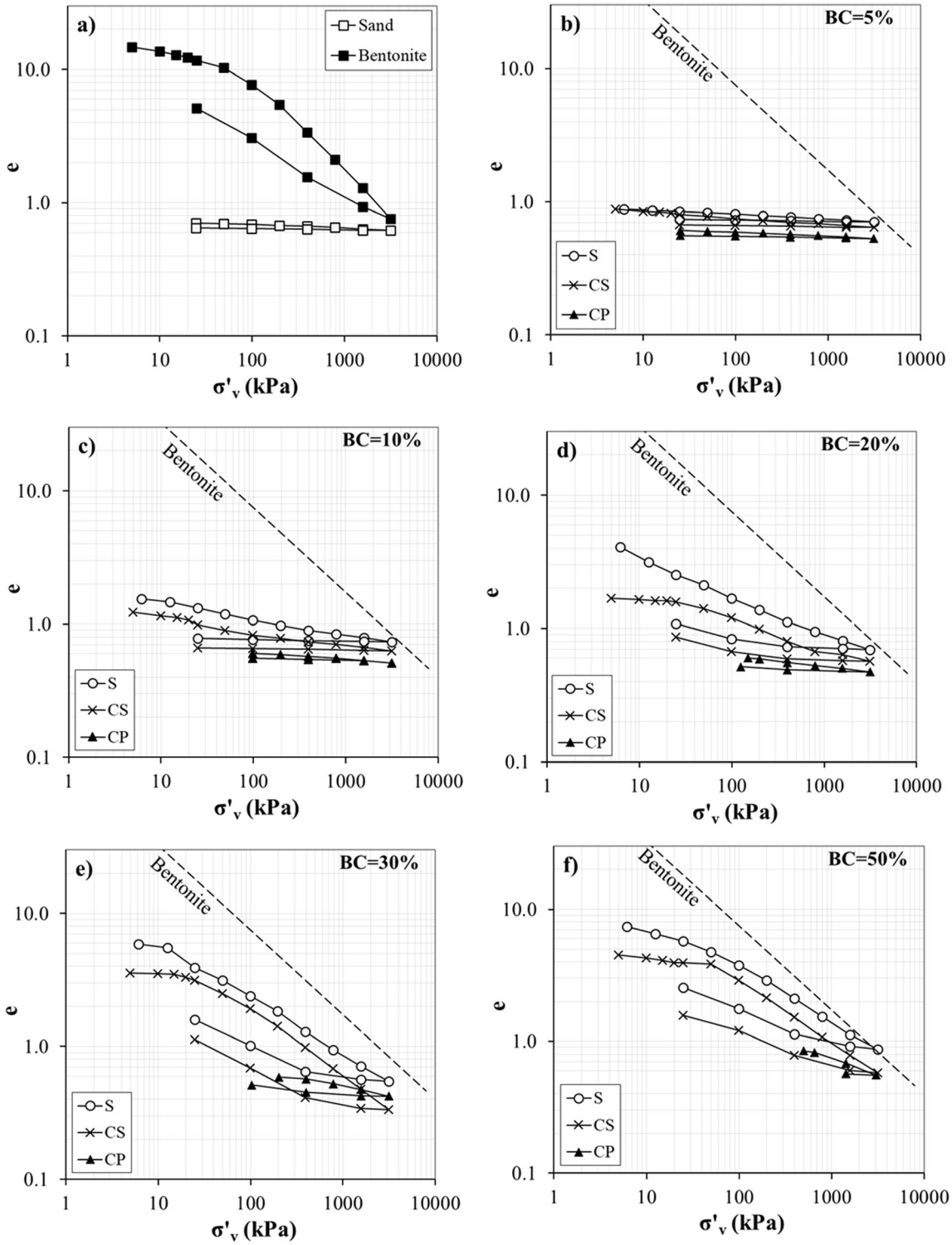

Fig. 12 Oedometer test results on samples left free to swell during saturation (CS) and on samples with compensated swelling during saturation (CP) (**a** sand and bentonite; **b** BC = 5%; **c** BC = 10%; **d** BC = 20%; **e** BC = 30%; **f** BC = 50%)

obtained on samples with prevented swelling (CP). Notably, after an initial portion, the curves for S and CS samples tend to be almost parallel, this response kept during both the primary loading and unloading paths. This evidence implies that the reconstitution process affects the fabric of materials. Compaction of the partially saturated mixes results in a void ratio gap but, at least for the considered stress levels, does not affect much compressibility, this

property dictated primarily by the bentonite content. The relative position of the curves confirms the evidence of Burland [5] who attributed the differences in the compression response of clayey materials to the different fabric induced by the reconstitution method.

In general, for low bentonite content (say less than 10%) compressibility is very low and primary loading and unloading curves are rather overlapped. On the contrary, there is a progressive detachment of the primary loading from the unloading curves and a clearer appearance of yielding for the S and CS curves. In other words, the overall soil response is similar to that of granular materials, i.e. slightly irreversible with a limited compressibility, for low BC values; response becomes similar to plastic soils for larger BC values. When BC increases, the curves tend to the upper bound represented by the ICL of the pure bentonite, i.e. presenting higher initial void ratio and compressibility index.

However, a difference must be noted in the initial portion of the curves for S and CS samples. While S samples present an almost straight line during primary loading, a knee typical of yielding becomes progressively sharper for BC larger than 20% on CS samples. A yielding stress p'_c approximately equal to 50–60 kPa can be identified for samples with BC > 20%. This result suggests that the compaction effort coupled with the matrix suction induced by the partial saturation of CS samples induces a sort of overconsolidation. This concept is clearly formulated into constitutive models [46] that postulate a double hardening mechanism with past stress history quantified by two summed contributions, volumetric strain and matrix suction.

The CP curves also start from initial higher void ratios with increasing BC, as an effect of the bentonite content on compaction (see Fig. 3). The suppression of swelling during saturation (see CP compared with CS curves) makes soil less compressible even for effective stresses exceeding the pressure applied during saturation. The differences between CS and CP curves can be explained considering that water saturation induces a relaxation of the matrix suction activated in the bentonite during compaction in the unsaturated state. In the case of free swelling, the applied total stress is zero throughout the wetting process and nil effective stresses are applied in the final saturated condition. This state enables the soil pores to dilate adsorbing water which is thereafter expelled during the subsequent oedometer compaction. In the prevented swelling, the reduction of matrix suction is simultaneously compensated by an increase of the total stresses in order to prevent expansion. Thus, the soil is progressively brought to its final effective stress state (variable with the bentonite content) without an unloading–reloading cycle but by a progressive transfer of stresses from matrix suction to external load. The observed differences can thus be explained with ageing. In fact, the saturation process and the simultaneous prevention of swelling lasted several weeks during which load was progressively increased up to the final values reported in Fig. 11. Leonards and Girault [24] (reported by Burland [5]) claim that the micro-fabric of a clay can develop increased resistance to compression during ageing and that this resistance does not depend on volume reduction due to creep. When aged clays are loaded, the structural resistance breaks down at a critical pressure and the subsequent compression curve is initially significantly steeper than the standard virgin line. The authors introduced the term 'quasi-preconsolidation pressure' to describe this critical pressure.

The dependency of the compressibility index on the bentonite content and sample formation is summarized in Fig. 13. For BC = 5%, the compressibility is very low and not influenced by the load path induced by the CS and CP reconstitution procedures. This result may be explained considering that the behaviour for such low BC values is governed by the sand matrix. For higher BC values, the compressibility increases for all cases, with similarly higher for CS and S, lower for CP loading path. The increase of compressibility proceeds with slower rates after BC = 30%, meaning that the role of sand on the soil compressibility becomes more marginal after this percentage.

As a conclusion, the most meaningful change of response between the two considered conditions occurs within the BC interval 10–30% (named transition phase in Fig. 4), while the role of coarse soil on the compressibility of material ceases when sand particles become floating in the bentonite matrix. It also follows from the performed tests that compressibility of the sand–bentonite layer is higher in case of saturation induced by rainwater before placing the waste and that prevention of swelling by the weight of wastes makes the material less compressible even when vertical stress exceeds the swelling pressure. The difference between the two conditions deserves to be

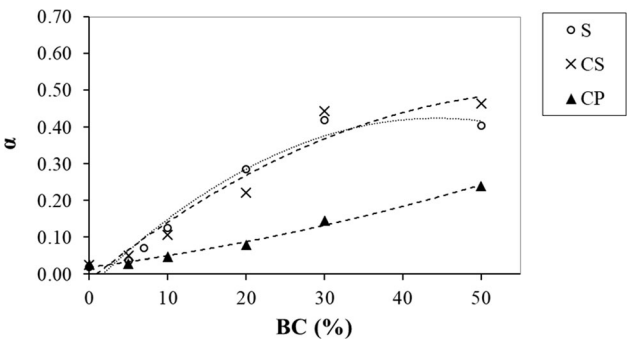

Fig. 13 Compressibility (α) versus bentonite content (BC) for different reconstitution processes

carefully evaluated as it could induce unforeseen stresses or strains paths in the waste disposal linings at the contact between zones undergoing different placement histories.

6 Permeability

The hydraulic conductivity of the mixtures k has been determined by oedometer compression tests, inferring the time-settlement curves with the classical one-dimensional consolidation theory of Terzaghi [48], i.e. computing the permeability through Eq. (4):

$$k = \frac{c_v \cdot \gamma_w}{E_{\text{oed}}} \tag{4}$$

where c_v is the vertical consolidation coefficient, γ_w the specific weight of water and E_{oed} the oedometric modulus ($\Delta\sigma'_v/\Delta\varepsilon_v$). The same procedure was applied by Sun et al. [45] to measure the permeability of saturated sand–bentonite mixtures.

The analysis has been performed on CS samples (Compacted-Swelled) and on samples prepared at a water content equal to 1 ÷ 1.5 times the liquid limit (S). However, inference of the tests on CP samples (compacted-prevented swelling) was rarely possible due to the irregular shape of the time–settlement curves.

The correlation k(e) is plotted in Fig. 14 for the CS and S samples prepared with three different bentonite contents (BCs, respectively, equal to 5, 50 and 100%). The comparison reveals a fairly good agreement of the data obtained with the two sample formation procedures, with the same linear relationship between log(k) and log(e) for each mixture and without a systematic difference. This outcome somehow confirms the evidence shown in previous studies [16, 21, 29, 59].

Moreover, it is pointed out that the hydraulic conductivity of a soil in unsaturated conditions is lower than the corresponding value (at the same void ratio) obtained on saturated soil. In fact, it is well known that permeability decreases as soil becomes unsaturated since less pore space is filled with water [15]. For instance, several studies carried out on compacted sand–bentonite mixtures show a decrease in hydraulic conductivity for the microstructural change during the saturation process [55] and a relationship of the hydraulic conductivity with the amount of bentonite, dry density of the mixture and water content at compaction [36, 41]. For this reason, the dependency of the hydraulic conductivity on the bentonite content has been evaluated on the S samples, i.e. on the samples formed with a very high water content that better guarantees saturation, and reported in the bi-logaritmic *e*–*k* plot of Fig. 15.

The hydraulic conductivity values of the pure sand, measured in previous direct permeability tests performed on the sand in a loose (e = 0.82, $k = 4.94 \cdot 10^{-5}$ m/s) and dense state (e = 0.51, $k = 3.82 \cdot 10^{-5}$ m/s), are reported for reference in the plot. As logically expected, and noticed by Sun et al. [45], permeability decreases with increasing BC values. However, even small percentages of bentonite (BC = 5%) provide a very low permeability to the saturated mixtures, able to satisfy the minimum value ($k_{\text{min}} = 10^{-9}$ m/s) usually required for the hydraulic barriers of landfills. These results can be seen in conjunction with the previously shown microstructural analysis. In particular, the function k–e shows different rates for the lowest (5 and 7%) and the largest BC (> 10%). This evidence can be related to the material's microstructure, dominated by the sand at the lower bentonite content (Fig. 7b), progressively more influenced by the finer soil (Fig. 7c–e). On the other side, the larger permeability of sand–bentonite mixtures compared with the pure bentonite can be related to the size

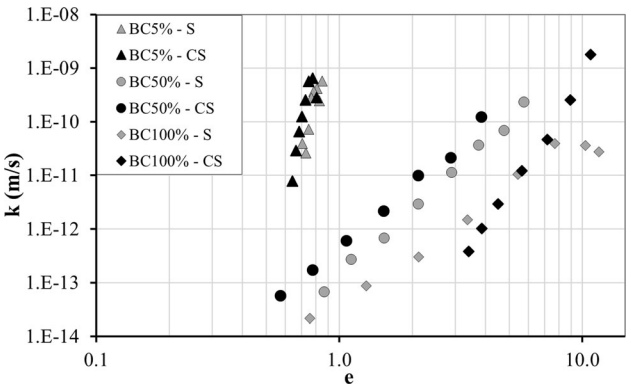

Fig. 14 Hydraulic conductivity versus void ratio for CS and S samples formed with different bentonite content

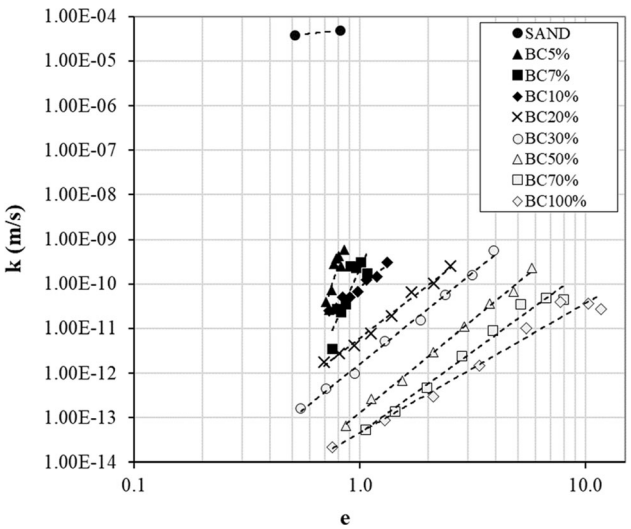

Fig. 15 Hydraulic conductivity of sand–bentonite mixtures in fully saturated condition

and amount of intra-grain and inter-cluster pores (Fig. 8a, b) that increases while reducing BC.

7 Conclusions

The experimental investigation has shown, in general, that the properties of the sand–bentonite mixtures are markedly influenced by the percentage of bentonite (i.e. bentonite content BC), as could otherwise be expected. In particular, three different structural types were observed after mechanical compaction to Proctor's optimum: a first structural type is obtained for low values of the bentonite content where the sandy matrix, being predominant, provides the mixture with a mechanical behaviour similar to that of an incoherent material; a second type is determined for high percentages of bentonite, since the grains of sand are dispersed in the clayey matrix which gives the mixture the mechanical behaviour typical of a fine-grained material; finally, a mixed structure occurs for intermediate compositions of the mixture, where both granulometric components contribute to the mechanical behaviour of the mixture itself.

The three possible types of microstructure identified in the compaction tests have been confirmed by means of a direct microstructural investigation (scanning electron microscopy and mercury intrusion porosimetry).

The permeability of the mixtures decreases significantly as the bentonite content increases and when the void ratio decreases during one-dimensional compression. It is noted, however, that even small percentages of bentonite (i.e. BC = 5%) provide a very low permeability to the mixtures which could satisfy the minimum value ($k_{min} = 10^{-9}$ m/s) usually required for the hydraulic barriers of landfills.

The compressibility of the compacted mixtures was also investigated, by means of numerous oedometer tests planned in order to simulate two different limit conditions that can occur at the bottom of a landfill. In the first limit case, it is assumed that the landfill bottom is wetted by rainwater before placing the waste and therefore the sand–bentonite layer can swell freely before being subjected to overloading. In the second limit case, it is assumed that landfill construction proceeds without the influx of meteoric water (or leachate) and that the imbibition occurs only subsequently, due to the deferred production of the leachate. Therefore, swelling induced by the imbibition is counteracted by the vertical loading of the waste.

The swelling mechanism, induced by saturation of the compacted samples, was evaluated for both stress-wetting paths previously recalled. It was thus found that both the volumetric expansion and the swelling pressure increase almost linearly as a function of the bentonite content. Even the compressibility, measured for both paths, increases markedly as a function of the bentonite content.

In conclusion, the results obtained by this investigation provide valuable indications on the possible use of sand–bentonite mixtures for the construction of confinement barriers to be placed at the bottom of waste landfills. The first design requirement to consider is the permeability of the barrier which must be usually lower than 10^{-9} m/s; this requirement was respected for all the sand–bentonite mixtures and therefore provides a positive indication.

It is also necessary, however, to consider the workability of the mixtures and their tendency to swell if saturated by water or leachate. To this end, it is suggested to keep the bentonite content lower than 10%, in order to reduce and possibly eliminate swelling.

The tendency to shrinkage due to drying of bentonite [11] remains, however, to be investigated, as it could determine the appearance of cracks in the confinement barrier if exposed to air and sun drying.

Anyway, the design of a sand–bentonite barrier should be based on appropriate laboratory investigations performed on the sand and bentonite to be actually used. Specific tests may also be conducted using solutions similar to the expected leachate.

Expected settlements of the barrier should be computed, in order to verify deformation compliance of the sand–bentonite mixture. As a general rule, the Authors suggest to keep the placement water content slightly on the wet side of the compaction curve in order to provide larger flexibility and also to reduce the swelling tendency of the bentonite.

The design should be finally verified on site, in order to optimize the construction process and verify the behaviour of the barrier through appropriate investigations and checks.

Acknowledgements The research leading to these results has received funding from Project "Ecosistema dell'innovazione—Rome Technopole" financed by EU in NextGenerationEU plan through MUR Decree n. 1051 23.06.2022—CUP H33C22000420001

Data availability Data sets generated during the current study are available from the corresponding author on reasonable request.

References

1. Agus SS, Schanz T (2005) Effect of shrinking and swelling on microstructures and fabric of a compacted bentonite-sand mixture. In: Proceedings of the international conference on problematic soils, (Cyprus: Eastern Mediterranean University Gazimağusa) pp. 543–550
2. Ameta NK, Wayal AS (2008) Effect of bentonite on permeability of dune sand. Electron J Geotech Eng 13:1–7
3. ASTM D2435-96 (1996) Standard test methods for one-dimensional consolidation properties of soils using incremental loading
4. ASTM D698-00a (2000) Standard test methods for laboratory compaction characteristics of soil using standard effort (12 400 ft-lbf/ft^3 (600 kN-m/m^3))
5. Burland JB (1990) On the compressibility and shear strength of natural clays. Géotechnique 40(3):329–378
6. Chalermyanont T, Arrykul S (2005) Compacted sand-bentonite mixtures for hydraulic containment liners. Songklanakarin J Sci Technol 27(2):313–323
7. Cui Y-J (2017) On the hydro-mechanical behaviour of MX80 bentonite-based materials. J Rock Mech Geotech Eng 9:565–574
8. Daniel DE (1993) Case histories of compacted clay liners and covers for waste disposal facilities. In: International conference on case histories in geotechnical engineering. Paper 2
9. Delage P, Marcial D, Cui YJ, Ruiz X (2006) Ageing effects in a compacted bentonite: a microstructure approach. Géotechnique 56(5):291–304
10. Dixon DA, Graham J, Gray MN (1999) Hydraulic conductivity of clays in confined tests under low hydraulic gradients. Can Geotech J 36:815–825
11. Dixon DA, Gray MN, Thomas AW (1985) A study of the compaction properties of potential clay-sand buffer mixtures for use in nuclear fuel waste disposal. Eng Geol 21:247–255
12. El Mohtar CS, Bobet A, Santagata MC, Drnevich VP, Johnston CT (2012) Liquefaction mitigation using bentonite suspensions. J Geotech Geoenviron Eng 139(8):1369–1380
13. Evans JC (1991) Geotechnics of hazardous waste control systems. In: Fang H-Y (ed) Foundation Engineering Handbook. Chapman & Hall, pp 750–777
14. Evans JC (1993) Vertical cutoff walls DE Daniel (Eds) In: Geotechnical practice for waste disposal. Chapman & Hall UK pp 430–454
15. Fredlund DG, Rahardjo H, Fredlund MD (2012) Un-saturated soil mechanics in engineering practice. Wiley
16. Gibson RE, England GL, Hussey MJL (1967) The theory of one-dimensional consolidation of saturated clays, I. finite non-linear consolidation of thin homo-geneous layers. Geotechnique 17:261–273
17. Head KH (1994) Manual of soil laboratory testing - Permeabililty, shear strenght and compressibility tests. John Wiley & Sons, Inc., New York Toronto
18. Holtz RD, Kovacs WD (1981) An introduction to geotechnical engineering. Prentice-Hall Inc., NJ
19. Iolli S, Modoni G, Chiaro G, Salvatore E (2015) Predictive correlations for the compaction of clean sands. Trans Geotech 4:38–49
20. Jappelli R, Silvestri T (2005) Questioni di Ingegneria Geotecnica. Helvenius, Benevento
21. Kenney TC, Veen WV, Swallow MA, Sungaila MA (1992) Hydraulic conductivity of compacted bentonite–sand mixtures. Can Geotech J 29(3):364–374
22. Komine H, Ogata N (1999) Experimental study on swelling characteristics of sand-bentonite mixture for nuclear waste disposal. Soils Found 39(2):83–97
23. Kutzner C (1997) Earth and rockfill dams: Principles for design and construction. CRC Press, UK
24. Leonards GA, Girault P (1961) A study of the one-dimensional consolidation test. In: Proc 5th Int Conf on Soil Mech Paris 1 213–219
25. Manca D (2015) Hydro-chemo-mechanical characterisation of sand/bentonite mixtures, with a focus on the water and gas transport properties. PhD Thesis. EPFL
26. Mitchell JK, Soga K (2005) Fundamentals of soil behaviour. John Wiley & Sons, Hoboken NJ
27. Mollins LH, Stewart DI, Cousens TW (1996) Predicting the properties of bentonitesand mixtures. Clay Miner 31(2):243–252
28. Montanez JEC (2002) Suction and volume changes of compacted sand-bentonite mixtures. (Doctoral dissertation, University of London)
29. Pane V, Croce P, Znidarcic D, Ko HY, Olsen HW, Schiffman RL (1983) Effects of consolidation on permeability measurements for soft clay. Technical Note. Geotechnique XXXIII, N.1
30. Polidori E (2003) Proposal for a new plasticity chart. Géotechnique 53(4):397–406
31. Polidori E (2009) Reappraisal of the activity of clays activity chart. Soils Found 49(3):431–441
32. Proia R (2018) Experimental analysis of sand-bentonite mixtures. PhD Thesis. University of Cassino and Southern Lazio
33. Proia R, Croce P, Modoni G (2016) Experimental investigation of compacted sand-bentonite mixtures. Procedia Eng 158:51–56
34. Pusch R (2015) Bentonite clay: environmental properties and applications. CRC Press
35. Romero E, Simms PH (2008) Microstructure investigation in unsaturated soils: a review with special attention to contribution of mercury intrusion porosimetry and environmental scanning electron microscopy. Geotech Geol Eng 26:705–727
36. Sällfors G, Öberg-Högsta AL (2002) Determination of hydraulic conductivity of sand-bentonite mixtures for engineering purposes. Geotech Geol Eng 20:65–80
37. Santagata M, Clarke JP, Bobet A, Drnevich VP, El Mohtar CS, Huang P-T, Johnston CT (2014) Rheology of concentrated bentonite dispersions treated with sodium pyrophosphate for application in mitigating earthquake-induced liquefaction. Appl Clay Sci 99:24–34
38. Santucci de Magistris F, Silvestri F, Vinale F (1998) Physical and mechanical properties of a compacted silty sand with low bentonite fraction. Can Geotech J 35(6):909–925
39. Shaker AA, Elkady TY (2016) Investigation of the hydraulic efficiency of sand-natural expansive clay mixtures. Int J Geomate 11(25):1790–1795
40. Shelley EO (2011) Some geotechnical properties to characterize Mexico city clay. In: Pan-Am CGS geotechnical conference
41. Shi FJ, Feng SJ, Zheng QT, Peng CH (2024) Hydraulic conductivity and compressibility of polyanionic cellulose-modified sand-calcium bentonite slurry trench cutoff wall materials. Acta Geotech 19(1):1–18. https://doi.org/10.1007/s11440-023-02112-y
42. Sivapullaiah PV, Sridharan A (1985) Liquid limit of soil mixtures. Geotech Test J 8(3):111–116
43. Srikanth V, Mishra AK (2016) A laboratory study on the geotechnical characteristics of sand–bentonite mixtures and the role of particle size of sand. Int J Geosynth Ground Eng 2(3):1–10
44. Studds PG, Stewart DI, Cousens TW (1998) The effects of salt solutions on the properties of bentonite-sand mixtures. Clay Miner 33(4):651–660
45. Sun WJ, Wei ZF, Liu SQ, Chen C, Zhang L, Sun DA (2016) Deformation characteristics and permeability of saturated bentonite-sand mixtures. In: Unsaturated soil mechanics—from theory to practice Taylor & Francis London pp 229–234

46. Tamagnini R (2004) An extended Cam-clay model for unsaturated soils with hydraulic hysteresis. Geotechnique 54(3):223–228
47. Tatsuoka F, Correia AG (2016) Importance of controlling the degree of saturation in soil compaction, Advances in transportation geotechnics. In: The 3rd Int. Conf on Transportation geotechnics (ICTG 2016) 143 pp 556–565
48. Terzaghi K (1943) Theory of consolidation. Theoretical soil mechanics. Wiley, pp 265–296
49. Thevanayagam S (1998) Effect of fines and confining stress on undrained shear strength of silty sands. J Geotech Geoenviron Eng 124(6):479–491
50. Thevanayagam S, Shenthan T, Kanagalingam T (2003) Role of intergranular contacts on mechanisms causing liquefaction & slope failures in silty sands. Final Report. (University at Buffalo, State University of New York, Department of Civil, Structural, and Environmental Engineering)
51. Thevanayagam S, Shenthan T, Mohan S, Liang J (2002) Undrained fragility of clean sands, silty sands, and sandy silts. J Geotech Geoenviron Eng 128(10):849–859
52. Vecellio P, Croce A (1957) La diga di terra di Castelsanvincenzo. Rivista Italiana Di Geotecnica 6:309–323
53. Villar MV, Lloret A (2004) Influence of temperature on the hydro-mechanical behaviour of a compacted bentonite. Appl Clay Sci 26(1–4):337–350
54. Wang DW, Zhu C, Tang CS, Li SJ, Cheng Q, Pan XH, Shi B (2021) Effect of sand grain size and boundary condition on the swelling behavior of bentonite–sand mixtures. Acta Geotech 16:2759–2773
55. Wang Q, Cui YJ, Tang AM, Barnichon JD, Saba S, Ye WM (2013) Hydraulic conductivity and microstructure changes of compacted bentonite/sand mixture during hydration. Eng Geol 164:67–76
56. Washburn EW (1921) Note on a method of determining the distribution of pore sizes in a porous material. Proc Natl Acad Sci USA 7:115–116
57. Zeng Z, Cui YJ, Talandier J (2021) Investigating the swelling pressure of highly compacted bentonite/sand mixtures under constant-volume conditions. Acta Geotech 1:8
58. Zimmie TF, Almaleh LJ (1976) Shrinkage of soil specimens during preparation for porosimetry tests In: Soil specimen preparation for laboratory testing—ASTM Special Technical Publication 599 pp. 202 215
59. Znidarcic D, Croce P, Pane V, Ko HY, Olsen HW, Schiffman RL (1984) The theory of one-dimensional consolidation of saturated clays: III. Exist-ing testing procedures and analyses. Geotechnical Testing Journal 7 3 123 Published by ASTM, Philadephia, U.S.A.